

## ARTICLE OPEN



## Uncertainties in tropical cyclone landfall decay

Kelvin T. F. Chan<sup>1,2,3</sup>, Johnny C. L. Chan<sup>4,5,6</sup>, Kailin Zhang<sup>1</sup> and Yue Wu<sup>1</sup>

Understanding the responses of landfalling tropical cyclones to a changing climate has been a topic of great interest and research. Among them, the recently reported slowdown of tropical cyclone landfall decay in a warming climate engenders controversy. Here, the global climatology of landfall decay, based on the tropical cyclone best-track data available, reveals that the reported trends are uncertain and not universal, but spatial, temporal, data, and methodology dependent such that any claim of a climate trend could be misleading at present. The effective area of moisture supply from the ocean, most likely determined by the landfalling track modes, is demonstrated to be an important factor for the decay. This study provides timely essential clarifications of the current contentious understanding.

*npj Climate and Atmospheric Science* (2022)5:93; <https://doi.org/10.1038/s41612-022-00320-z>

## INTRODUCTION

Tropical cyclones are one of the most destructive natural disasters around the world, causing significant economic losses and casualties to the coasts and inland proximity when they make landfall. Their destructive potentials to the coastal regions are found to be increasing in the past decades<sup>1–11</sup> and could keep increasing in a warming climate<sup>3,4,7,10</sup>. Particularly, Li and Chakraborty<sup>7</sup> (hereafter LC<sup>7</sup>) recently reported a significant slowdown of the decay of North Atlantic landfalling hurricanes during 1967–2018. They showed that the contemporaneous rise in sea surface temperature is the primary cause that lengthens the decay time and suggested that the inland decay would become slower in a warming world. Song et al.<sup>8</sup> (hereafter SK<sup>8</sup>) followed LC<sup>7</sup> and showed that there is also a significant slowdown of the decay of the western North Pacific landfalling tropical cyclones on the Asian continent during 1966–2018. However, they suggested that it is more likely caused by the changes in the dynamic rather than thermodynamic variables. Later, Chan et al.<sup>12</sup> (hereafter CZ<sup>12</sup>) pointed out the calculation inadequacies<sup>13</sup> and questioned the methodology and robustness in LC<sup>7</sup> such that the reported slower decay over the past half-century may be exaggerated, although Li and Chakraborty argued otherwise<sup>14</sup>. Additionally, CZ<sup>12</sup> proposed that the decay highly depends on the landfalling track modes rather than the sea surface temperature, with the effective area of moisture supply from the ocean playing a vital role. Meanwhile, Phillipson and Toumi<sup>15</sup> also did not find a corresponding significant decrease in either exponential or algebraic landfall decay constants, which is in disagreement with LC<sup>7</sup>.

Hence, is the slowdown of the decay of landfalling tropical cyclones evident and globally similar? This study, a follow-up of CZ<sup>12</sup>, systematically reveals the global climatology of the landfall decay of tropical cyclones, clarifying the current confusion in the subject.

Time series of season-level (season-mean or annual-mean) and event-level decay timescale  $\tau$  in individual basins are shown in Figs. 1 and 2, respectively, based on the authoritative tropical cyclone best-track data available (see Methods). The global climatology shows that the trends of tropical cyclone landfall decay are spatial (basins), temporal (study periods), data (data

sources), and methodology (landfall event selection criteria such as landfall intensity thresholds and land-sea mask resolutions, and statistical techniques) dependent.

## RESULTS

## Basin-dependent

Trends of landfall decay vary among basins (Fig. 1). Given the same study period, some are increasing while some are decreasing. Meanwhile, some are statistically significant whereas some are not. For example, during 1967–2020, a significant increasing trend ( $0.42 \text{ h yr}^{-1}$ ,  $p < 0.05$ ) is found for North Atlantic tropical cyclones with landfall intensity  $\geq 64 \text{ kt}$ , while the trends in other basins are insignificant ( $p > 0.05$ ) or even decreasing over the similar study period. The reported slowdowns in tropical cyclone landfall decay<sup>7,8</sup> are therefore not a worldwide phenomenon<sup>15</sup>.

## Data-dependent

Given the same study period, different sources of best-track data can exhibit different trends even in the same basin (Fig. 1). For example, a significant decreasing trend ( $-0.3 \text{ h yr}^{-1}$ ,  $p < 0.01$ ) is found for the western North Pacific tropical cyclones with landfall intensity  $\geq 34 \text{ kt}$  during 1945–2019 using the JTWC best-track data, however, the corresponding trend diminishes and becomes insignificant ( $-0.03 \text{ h yr}^{-1}$ ,  $p = 0.75$ ) during 1950–2019 using the CMA best-track data. Likewise, during 1980–2019, a significant decreasing trend ( $-0.6 \text{ h yr}^{-1}$ ,  $p < 0.01$ ) is found from the western North Pacific tropical cyclones with landfall intensity  $\geq 64 \text{ kt}$  using the CMA best-track data, but the corresponding trend diminishes and becomes insignificant ( $-0.35 \text{ h yr}^{-1}$ ,  $p = 0.15$ ) using the JTWC best-track data. These inconsistencies are very likely due to the heterogeneities of operational procedures between the agencies, particularly the discrepancies in the estimation of tropical cyclone intensity<sup>16,17</sup>.

<sup>1</sup>School of Atmospheric Sciences, Sun Yat-sen University, and Southern Marine Science and Engineering Guangdong Laboratory (Zhuhai), Zhuhai, China. <sup>2</sup>Guangdong Province Key Laboratory for Climate Change and Natural Disaster Studies, Sun Yat-sen University, Zhuhai, China. <sup>3</sup>Key Laboratory of Tropical Atmosphere-Ocean System (Sun Yat-sen University), Ministry of Education, Zhuhai, China. <sup>4</sup>School of Energy and Environment, City University of Hong Kong, Hong Kong, China. <sup>5</sup>Shanghai Typhoon Institute, China Meteorological Administration, Shanghai, China. <sup>6</sup>Asia-Pacific Typhoon Collaborative Research Center, Shanghai, China. ✉email: chenth25@mail.sysu.edu.cn

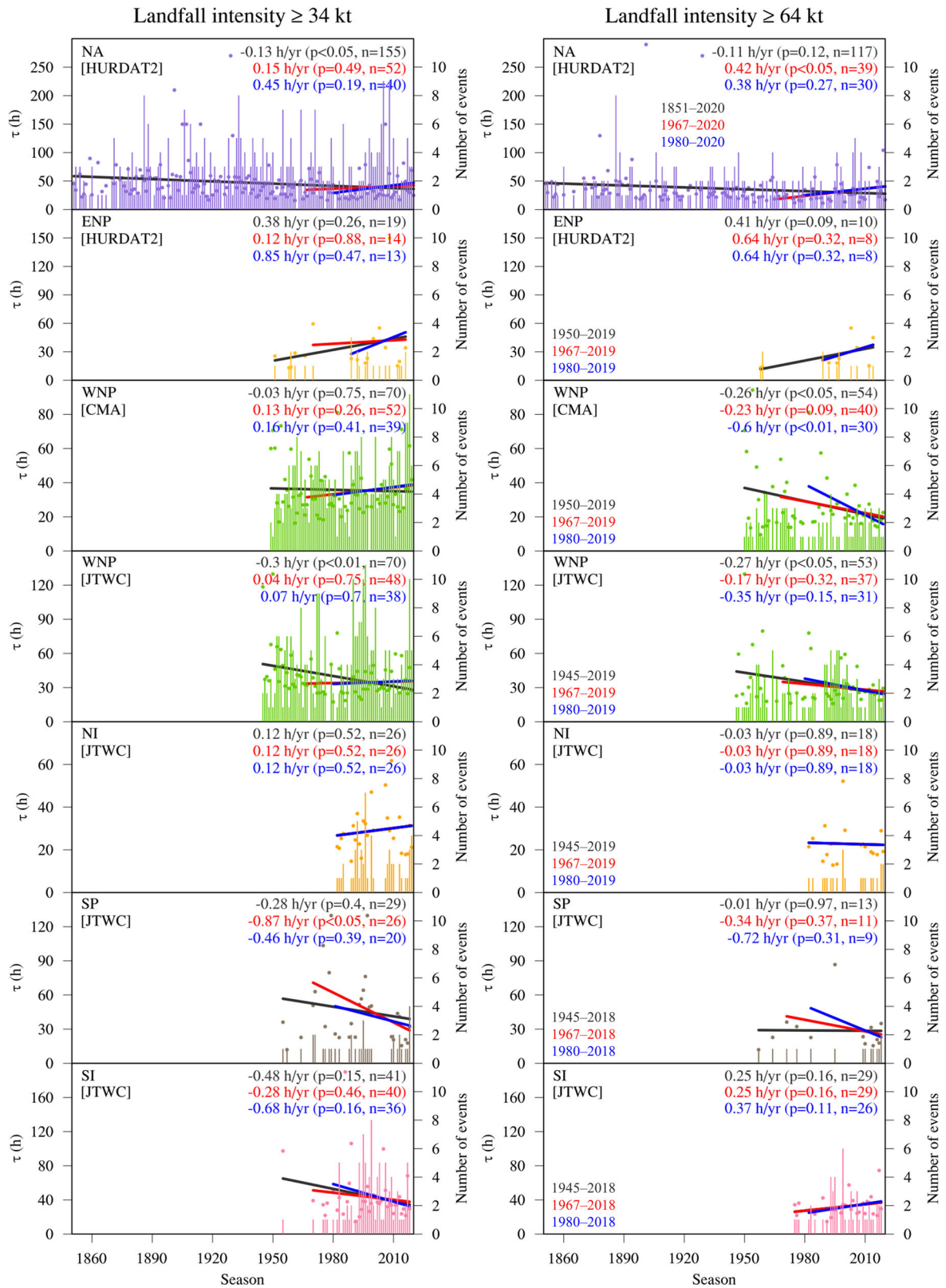


**Fig. 1** Global climatology of the season-level decay of landfalling tropical cyclones. Left and right columns show the time series of the season-level  $\tau$  (dots) and numbers of landfall events (bars) of tropical cyclones from individual basins with landfall intensity  $\geq 34$  kt and  $\geq 64$  kt, respectively (NA North Atlantic; WNP western North Pacific; NI North Indian Ocean; SP South Pacific; SI South Indian Ocean). Corresponding linear regression trends (lines),  $p$  values, and number of seasons  $n$  over different study periods are provided.

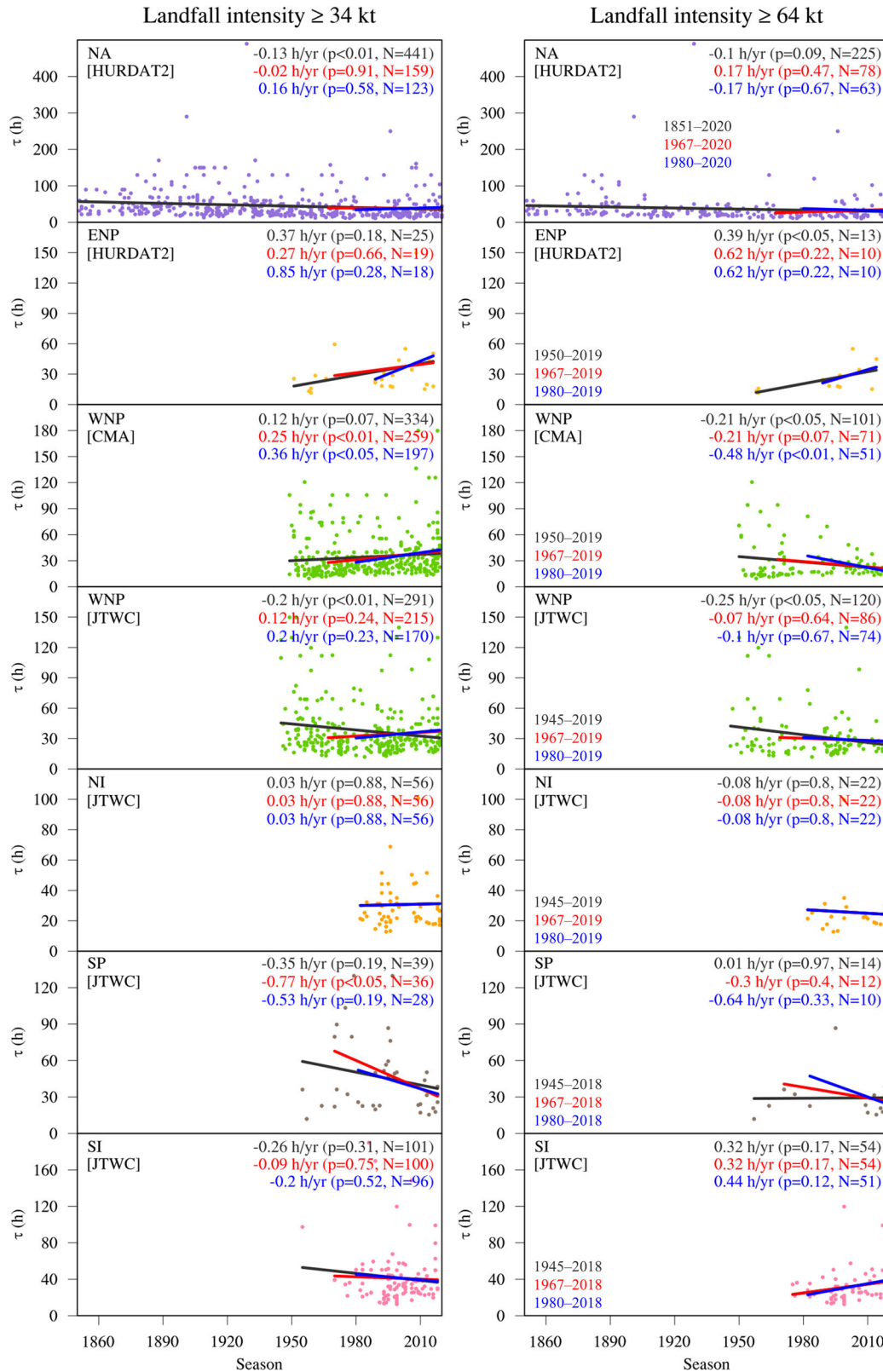


**Fig. 2** Global climatology of the event-level decay of landfalling tropical cyclones. Left and right columns show the time series of the event-level  $\tau$  (dots) and numbers of landfall events (bars) of tropical cyclones from individual basins with landfall intensity  $\geq 34$  kt and  $\geq 64$  kt, respectively (NA North Atlantic; WNP western North Pacific; NI North Indian Ocean; SP South Pacific; SI South Indian Ocean). Corresponding linear regression trends (lines),  $p$  values, and number of events  $N$  over different study periods are provided.

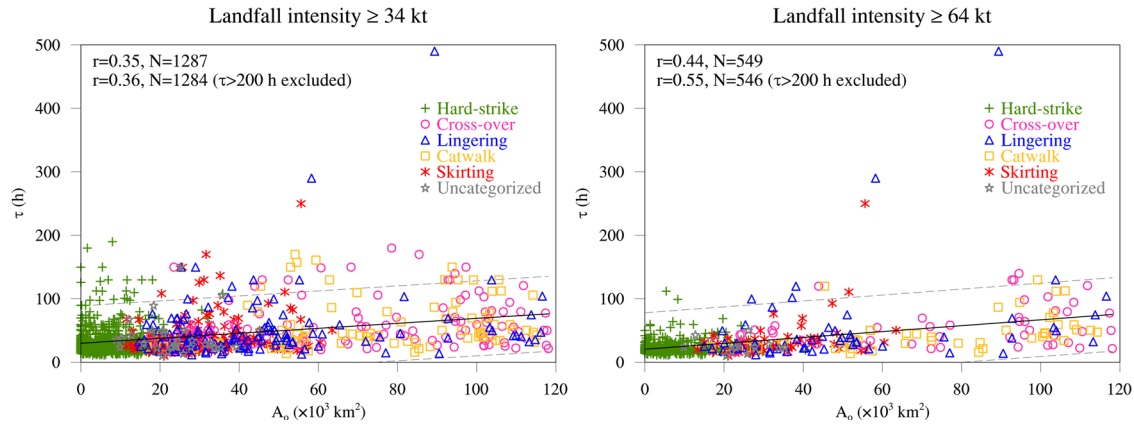


**Fig. 3 Global landfalling tropical cyclone track modes, effective area of moisture supply from the ocean  $A_o$ , and decay.** Scatter plots of event-level  $\tau$  versus  $A_o$  of tropical cyclones with landfall intensity  $\geq 34$  kt and  $\geq 64$  kt are shown in left and right panels, respectively. Corresponding correlations  $r$  and number of events  $N$  are provided. Linear regression lines (solid lines), and their corresponding 95% prediction bands (dash lines) derived from all events are overlaid.

### Study period-dependent

Even within the same basin and from the same data source, the trends and their corresponding significances are not consistent with time, but study-period dependent. Remarkably, some trends are even reversed. For instance, the decreasing trend during 1851–2020 in North Atlantic becomes increasing during 1967/80–2020 (Fig. 1). Similarly, the decreasing trend during 1945/50–2019 of the western North Pacific tropical cyclones with landfall intensity  $\geq 34$  kt becomes increasing during 1967/80–2019. These results suggest that large decadal to multi-decadal variations may exist. Hence, which period should be adopted to identify possible trends in a warming world? There is no absolute answer. Even if we follow the most-accepted approach to use the best-track data since the global satellite era (1980 onwards) that has been recognized to be more reliable<sup>18,19</sup>, the corresponding trends are found to be diverse among the basins and mostly insignificant (except the one deduced from the western North Pacific tropical cyclones with landfall intensity  $\geq 64$  kt retrieved from the CMA best-track data).

### Landfall intensity-dependent

Trends are sensitive to the landfall events conditioned by the thresholds of landfall intensity (Fig. 1 and see Methods). For example, during 1967–2020, the trend deduced from North Atlantic tropical cyclones with landfall intensity  $\geq 64$  kt is significantly increasing ( $0.42 \text{ h yr}^{-1}$ ,  $p < 0.05$ ), while the corresponding trend deduced from those with landfall intensity  $\geq 34$  kt is insignificant ( $0.15 \text{ h yr}^{-1}$ ,  $p = 0.49$ ). Likewise, during 1967/80–2019, the trends deduced from the western North Pacific tropical cyclones with landfall intensity  $\geq 34$  kt are increasing, while the trends deduced from those with landfall intensity  $\geq 64$  kt are decreasing. This implies that the trends are heavily subjected to the selection criteria of landfall events.

### Land-sea mask-dependent

In contrast to SK<sup>8</sup>, the increasing season-level  $\tau$  trends deduced from the western North Pacific tropical cyclones with landfall intensity  $\geq 34$  kt retrieved from the CMA and JTWC best-track data are not significant in this study (Fig. 1). These discrepancies are mainly due to the different selections of landfall events conditioned by the different resolutions of the land-sea mask (SK<sup>8</sup>: 1.25°; this study: 0.1°; see Methods), which supports CZ<sup>12</sup>. Many of the first points, or even the rest three points, of the landfall events in SK<sup>8</sup> are actually over the sea, thus altering the

target events of the study (i.e., the events over the land) and subsequently the trend analyses.

### Statistical technique-dependent

Trends deduced from the season-level  $\tau$  and event-level  $\tau$  are different (cf. Figs. 1 and 2), where the former is equally weighted in every season no matter how many landfalls occurred in each season while the latter is weighted by the landfall frequency. For example, the significant increasing trend deduced from North Atlantic tropical cyclones with landfall intensity  $\geq 64$  kt at season-level ( $0.42 \text{ h yr}^{-1}$ ,  $p < 0.05$ ) becomes insignificant at event-level ( $0.17 \text{ h yr}^{-1}$ ,  $p = 0.47$ ) during 1967–2020. Similarly, the insignificant increasing trends deduced from the western North Pacific tropical cyclones with landfall intensity  $\geq 34$  kt at season-level ( $0.13$ – $0.16 \text{ h yr}^{-1}$ ,  $p > 0.05$ ) become significant at event-level ( $0.25$ – $0.36 \text{ h yr}^{-1}$ ,  $p < 0.05$ ) during 1967/80–2019 based on the CMA best-track data.

Noticeably, the results inferred from the event-level  $\tau$  share all the aforementioned dependencies concluded from the season-level  $\tau$ . This suggests that no matter which statistical technique is employed, the trends are yet sensitive to the basins, data, study periods, landfall intensity thresholds, and land-sea mask resolutions.

## DISCUSSION

The analyses presented above clearly highlight the uncertainties and non-uniqueness of the reported slowdown trends of landfall decay of tropical cyclones in a warming world, which were derived from one or two snapshots in time or space. Any potential trend should be based on a comprehensive analysis, especially for tropical cyclones in the eastern North Pacific, North Indian Ocean, and South Pacific where the sample sizes are small.

Notably, if the contemporaneous rise in the sea surface temperature suggested by LC<sup>7</sup> is the main cause that lengthens the decay time in a warming world, a worldwide consistent slowdown decay trend should appear, which obviously is not the case. The sea surface temperature effect on the decay is therefore not universal or less pronounced. Instead, the globally significant positive  $A_o$ – $\tau$  relationship confirms that the effective oceanic area of moisture supply  $A_o$ , most likely governed by the landfalling track modes (see Methods), is a main and generic factor that determines the landfall decay<sup>12</sup> (Fig. 3). Landfalling tropical cyclones in the non-“hard-strike” modes have larger  $A_o$  than those in the “hard-strike” mode. The larger the  $A_o$ , the less the land surface friction and the less energy dissipated, and thus, a longer  $\tau$ .

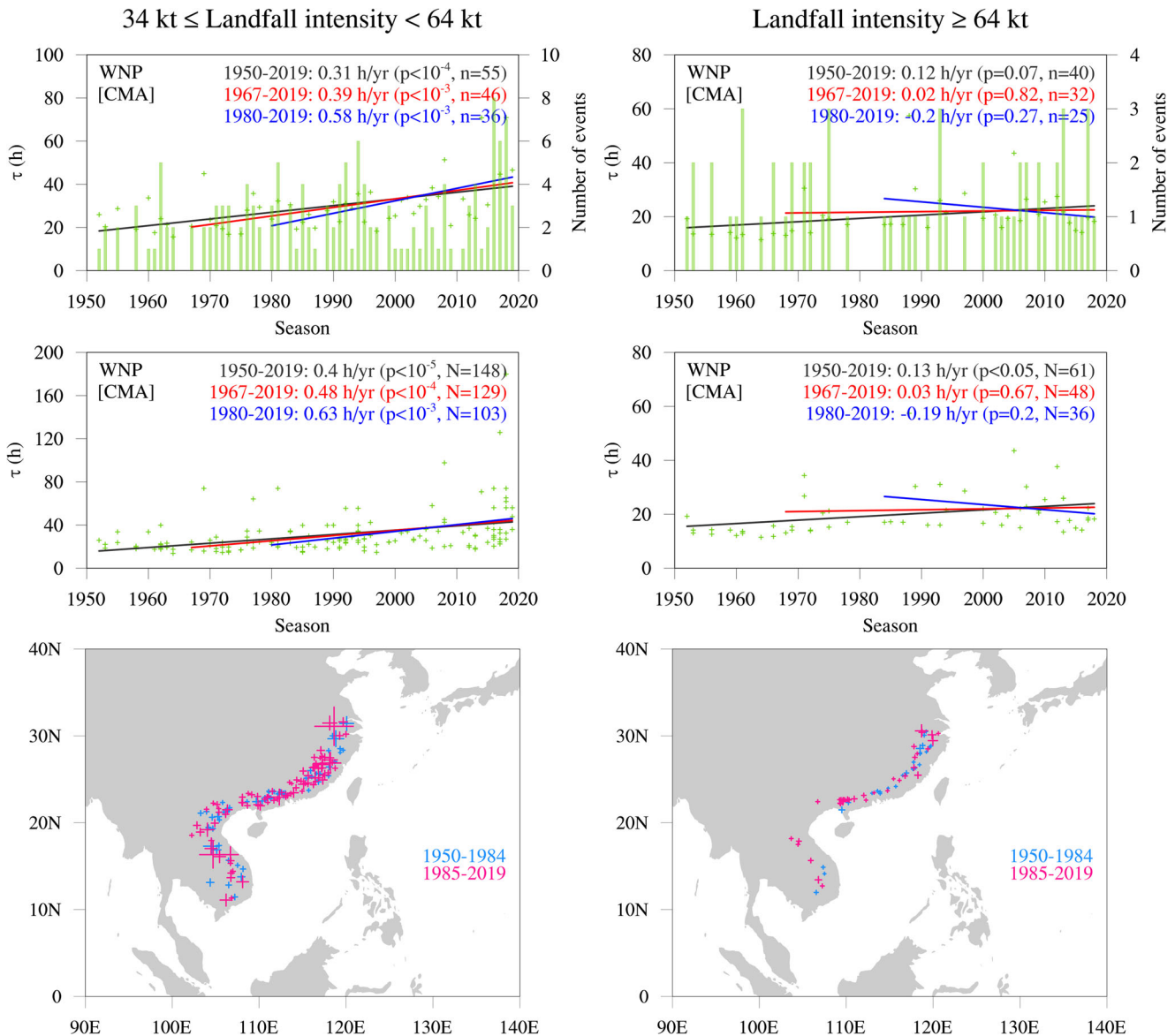


**Fig. 4** Global climatology of “hard-strike” decay of the western North Pacific landfalling tropical cyclones on China and Indochina. Left panels show the results from the weak “hard-strike” events with landfall intensity between 34 and 64 kt, while right panels show the results from the strong “hard-strike” events with landfall intensity  $\geq 64$  kt. Top and middle panels show the time series of the season-level  $\tau$  and event-level  $\tau$ , respectively. Corresponding linear regression trends over different study periods (lines) and numbers of landfall events (bars) are overlaid. Bottom panels show the spatial distributions of landfall events. Each marker represents the centroid position (the mean of tropical cyclone positions at four synoptic times past landfall) of an event, with its size proportional to the corresponding  $\tau$ .

Meanwhile, a larger  $A_0$  implies more sea surface enthalpy flux so that more thermal energy is available for kinetic energy conversion, and the decay would slow down as a result.

Subtly, Fig. 3 shows a discernible increase in correlation from the events with landfall intensity  $\geq 34$  kt ( $r = 0.35$ – $0.36$ ) to those with landfall intensity  $\geq 64$  kt ( $r = 0.44$ – $0.55$ ), suggesting that the strengthened positive  $A_0$ – $\tau$  relationship is largely attributed to the removal of weak landfalling tropical cyclones with landfall intensity between 34 and 64 kt. Among these weak landfalling tropical cyclones, some decay slowly over small  $A_0$ , while some decay very fast over large  $A_0$ , but the reasons leading to such a large variance could be a combination of the following. First, the less-organized structure of a weak landfalling tropical cyclone introduces uncertainties. The associated eyewall, wind circulation, and even the lower-tropospheric low-pressure center are often difficult to be observed or identified. Second, weak landfalling tropical cyclones possess small inertial stability such that they are

readily influenced by environmental perturbations (e.g., vertical wind shear and moisture advection) and underlying surface (e.g., surface roughness and moisture availability). Third, the advancement of science and technology (e.g., higher sensitivity and accuracy of measuring instruments), and the increase in inland observations (e.g., broader network of weather stations and radars) over recent decades could prolong the best-track records. In particular, the weak “hard-strike” western North Pacific tropical cyclones that made landfall on China and Indochina are found to last significantly longer over the past decades based on the CMA best-track data (Fig. 4), while the strong “hard-strike” ones did not. Meanwhile, Fig. 4 also shows that the weak “hard-strike” records were getting more and tracked farther inland, but not the strong “hard-strike” records.

Landfalling track modes are evidently subjected to the peripheral large-scale steering flow associated with the subtropical high (Fig. 5). The weakening (eastward retreat) of subtropical

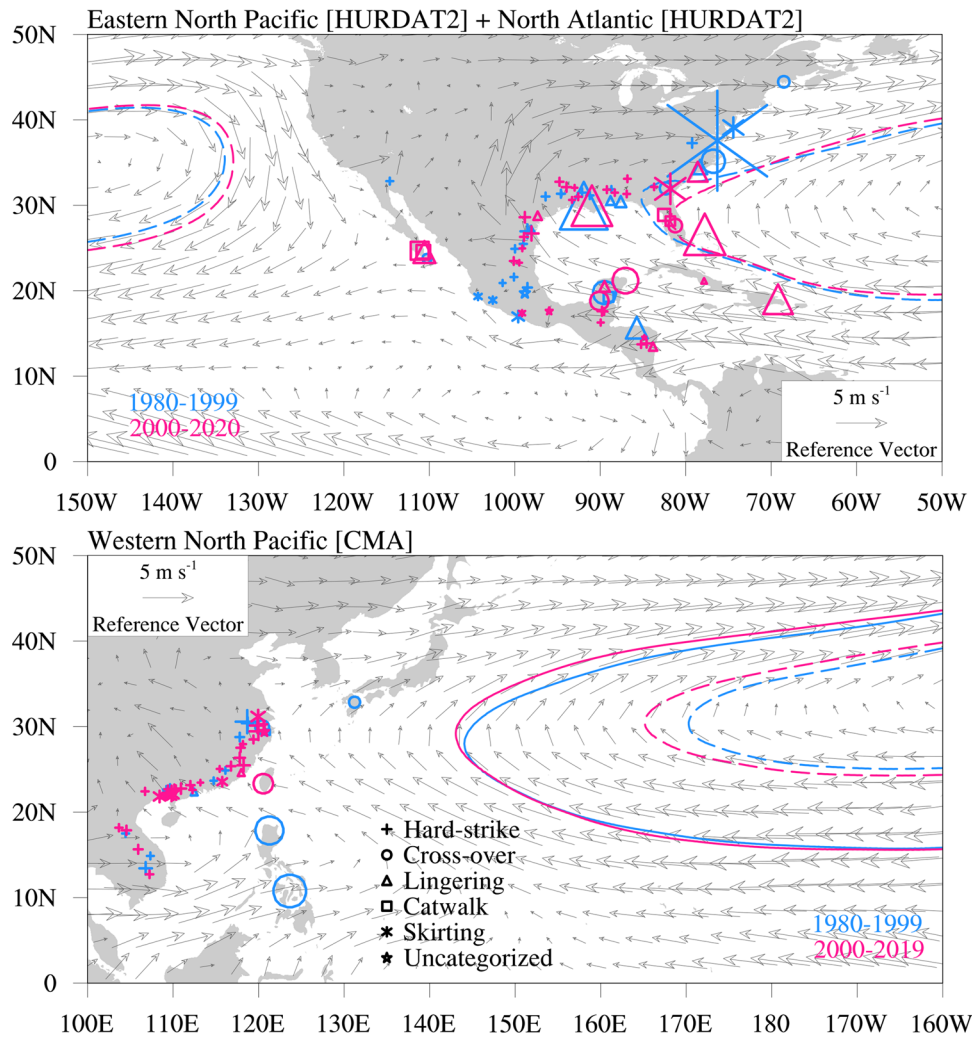


**Fig. 5 Variations of subtropical highs and spatial distributions of landfalling track modes since global satellite era (1980–2019/20).** Variations of subtropical highs are depicted by the 1520 geopotential height line (dash) at 850 hPa over the eastern North Pacific and North Atlantic, and by the 1490 (solid) and 1520 (dash) geopotential height lines at 850 hPa over the western North Pacific, with 40-yr mean wind vectors (July–October during 1980–2019) overlaid. Each marker represents the centroid position (the mean of tropical cyclone positions at four synoptic times past landfall) of an event in a particular landfalling track mode (specified in bottom panel; see Methods) with landfall intensity  $\geq 64$  kt, with its size proportional to the corresponding  $\tau$ .

high over the North Atlantic shifts the tropical cyclone activity eastward such that more tropical cyclones made landfall on Caribbean Islands, Yucatan Peninsula, Florida, and United States East Coast in the non-“hard-strike” modes. This is consistent with the increase in  $\tau$  of strong North Atlantic landfalling tropical cyclones (landfall intensity  $\geq 64$  kt) over the recent decades (Fig. 1). Conversely, the strengthening (westward extension) of the subtropical high over the western North Pacific shifts the tropical cyclone activity westward, which is consistent with the westward shift of the western North Pacific tropical cyclone tracks found during 1982–2018<sup>11</sup>, resulting in more “hard-strike” landfall events on China. This agrees well with the decrease in  $\tau$  of strong western North Pacific landfalling tropical cyclones (landfall intensity  $\geq 64$  kt; Figs. 1 and 2) over the past decades. The attribution to the change of North Atlantic subtropical high is not yet clear whereas that over the western North Pacific is suggested to be partly due to the atmospheric response to the observed Indian Ocean–western Pacific warming<sup>20</sup>.

This study provides a systematic and comprehensive evaluation of the global landfall decay of tropical cyclones in a warming world, providing timely essential clarifications of the current contentious understanding. Any claim of a universal climate trend

could be misleading at present. The results, however, do not rule out any possible long-term trends. In addition, it is likely that  $\tau$  may undergo large decadal to multidecadal variations (e.g., Atlantic Multidecadal Oscillation<sup>10</sup>) so that any trend that may be present due to global warming may not be identifiable. From a mitigation and adaptation point of view, attempts should also be made to identify such periodicities rather than a linear trend. Further analysis, particularly of larger best-track datasets with longer records and of higher consistency among operational tropical cyclone intensity estimates from different agencies, may yield a better understanding. For future projections, a careful examination and comparison of the results from the multi-high-resolution climate models is warranted.

## METHODS

### Data

Considering the coverage, availability, and reliability of the tropical cyclone best-track data, the United States National Hurricane Center data (HURDAT2)<sup>21</sup>, and the China Meteorological Administration (CMA) and the Joint Typhoon Warning Center (JTWC) data from the International Best Track Archive for Climate

Stewardship (IBTrACS) data<sup>22</sup>, including tropical cyclone positions and maximum sustained winds, are adopted (Supplementary Table 1). In the western North Pacific, given the numbers of identified tropical cyclone landfalls in the Japan Meteorological Agency (JMA) and the Hong Kong Observatory (HKO) data are much smaller than those in the CMA and JTWC best-track data, the JMA and HKO best-track data are not used<sup>8</sup>. In addition, to be homogeneous with other basins as far as possible, the JTWC best-track data are employed for South Indian Ocean and South Pacific, while those from the Australian Bureau of Meteorology, the Fiji Meteorological Service, and the Metrological Service of New Zealand are not taken. Note that the tropical cyclone season in the Northern Hemisphere starts from January and ends in December in each year, whereas that in the Southern Hemisphere is from July to following June.

The monthly fifth generation of European Center for Medium-Range Weather Forecasts (ECMWF) atmospheric reanalysis of the global climate<sup>23</sup> (ERA5;  $0.25^\circ \times 0.25^\circ$ , 1980–2020) is used to examine the winds and the subtropical high. The ERA5 is recognized to be one of the mainstream reanalysis datasets that has been widely using in operation and research. The ERA5 provides hourly estimates of a large number of atmospheric, land, and oceanic climate variables. The data covers the Earth on a 30 km grid and resolves the atmosphere using 137 levels from the surface up to a height of 80 km.

The 1 arc-minute global relief model of Earth's surface that integrates land topography and ocean bathymetry (ETOPO1) data is used to determine the land-sea mask. Given the uncertainty in the estimation of tropical cyclone center, the ETOPO1 data is firstly regridded to  $0.1^\circ$  resolution (a precision of the best-track position data) using bilinear interpolation. Secondly, the nearest 9 points (centered at the best-track position) are retrieved to determine whether the tropical cyclone is over the land or over the sea. If there are  $\geq 3$  points that the relief data are  $\geq -1$  m, the tropical cyclone is considered to be over the land. This approach is more applicable than those in LC<sup>7</sup> and CZ<sup>12</sup> because it increases the buffer for landfall determination such that it can count the landfalling tropical cyclones that are close to the rigid landmass as landfall. In addition, it can filter the samples that are on small islands and on small inland water (e.g., lakes and rivers). Note that the  $1.25^\circ$  land-sea mask resolution in SK<sup>8</sup> is rather loose that includes many events over the sea, the inclusion of which contaminates the target events of the study (i.e., the events over the land). Moreover, the coarse resolution of land-sea mask substantially alters the effective oceanic area of moisture supply  $A_o$  defined in this study.

### Landfall event

Three criteria are specified for determining a landfall event. First, two thresholds of landfall intensity are conditioned: (1) the intensity of the first inland data point  $\geq 34$  kt, the minimum intensity for gale force according to the Beaufort wind scale; (2) following LC<sup>7</sup> and CZ<sup>12</sup>, the intensity of the first inland data  $\geq 64$  kt, the minimum intensity for hurricane force according to the Saffir–Simpson scale. Excluding the landfall events below hurricane force can subtly filter out the weak tropical cyclones that may not be well observed or estimated over the land, especially those in the early stage (before 1980s) when the automatic weather stations, radars, and satellites were not well established, developed, and networked. Second, there are at least four continuous synoptic (0000, 0600, 1200, and 1800 UTC) inland data points. This can exclude the tropical cyclones that stay over the land  $< 18$  h<sup>7,8,12</sup>. Third, to reduce the influence from atypical events, those that underwent intensification, no change in intensity, or extratropical transition in the first 18 h past landfall are filtered<sup>7,8,12</sup>.

### Study periods

To be informative, comparative, and conservative, three study periods are examined. First: the period since the start of best-track data; second: the period since the start of study periods in LC<sup>7</sup>, SK<sup>8</sup>, and CZ<sup>12</sup> (1967 onwards); and third: the period since the global satellite era (1980 onwards). These help in examining the persistency of trend with time.

### Decay timescale $\tau$

The calculation of  $\tau$  follows LC<sup>7</sup> and CZ<sup>12</sup>. The tropical cyclone intensity ( $V$ ) is assumed to exhibit an exponential decay<sup>24</sup> as  $V(t) = V(0)e^{-t/\tau}$ , where  $t$  is the time past landfall. The first four continuous synoptic inland data points are extracted to fit the  $\tau$  by regression. A larger  $\tau$  suggests a slower inland decay, and vice versa.

### Effective oceanic area of moisture supply $A_o$

Following CZ<sup>12</sup>,  $A_o$  is defined as the average oceanic area within 200-km radius from the tropical cyclone center from the second to fourth synoptic times past landfall.

### Landfalling track modes

The categorization of landfalling track modes basically follows CZ<sup>12</sup> (Supplementary Fig. 1). Based on the characteristics of landfalling tracks, landfall events are grouped into two modes: “hard-strike” and non-“hard-strike”, with the latter further categorized into “cross-over”, “lingering”, “catwalk”, and “skirting” modes. “Hard-strike” mode categorizes hurricanes making direct landfall and experiencing paltry air-sea interaction after. “Cross-over” mode categorizes hurricanes making landfall across the landmass. “Lingering” mode categorizes hurricanes making landfall by lingering along the coast. “Catwalk” mode categorizes hurricanes making landfall along the long and narrow landmass. “Skirting” mode categorizes hurricanes making landfall by skirting the coastline.

This method categorizes over 98% of landfall events while the remaining 2% are uncategorized which belong to the non-“hard-strike” mode. No matter how these  $< 2\%$  events are further categorized, the main conclusions of the study are not altered.

### DATA AVAILABILITY

The HURDAT2 best-track data<sup>21</sup> is available at <https://www.nhc.noaa.gov/data/>. The JTWC and CMA best-track data are extracted from the IBTrACS data<sup>22</sup> which is available at <https://www.ncdc.noaa.gov/ibtracs/>. The ERA5 reanalysis<sup>23</sup> is available at <https://www.ecmwf.int/en/forecasts/datasets/reanalysis-datasets/era5>. The ETOPO1 relief data is available at <https://doi.org/10.7289/V5C8276M>. Data that supports the findings of this study is available from the corresponding author on request.

### CODE AVAILABILITY

The codes that support the findings of this study are available from the corresponding author on request.

Received: 26 May 2022; Accepted: 4 November 2022;  
Published online: 17 November 2022

### REFERENCES

- Chen, X., Wu, L. & Zhang, J. Increasing duration of tropical cyclones over China. *Geophys. Res. Lett.* **38**, L02708 (2011).
- Weinkle, J., Maue, R. & Pielke, R. Jr. Historical global tropical cyclone landfalls. *J. Clim.* **25**, 4729–4735 (2012).
- Mendelsohn, R., Emanuel, K., Chonabayashi, S. & Bakkensen, L. The impact of climate change on global tropical cyclone damage. *Nat. Clim. Change* **2**, 205–209 (2012).
- Woodruff, J. D., Irish, J. L. & Camargo, S. J. Coastal flooding by tropical cyclones and sea-level rise. *Nature* **504**, 44–52 (2013).

5. Mei, W. & Xie, S.-P. Intensification of landfalling typhoons over the northwest Pacific since the late 1970s. *Nat. Geosci.* **9**, 753–757 (2016).
6. Liu, L., Wang, Y., Zhan, R., Xu, J. & Duan, Y. Increasing destructive potential of landfalling tropical cyclones over China. *J. Clim.* **33**, 3731–3743 (2020).
7. Li, L. & Chakraborty, P. Slower decay of landfalling hurricanes in a warming world. *Nature* **587**, 230–234 (2020).
8. Song, J., Klotzbach, P. J., Zhao, H. & Duan, Y. Slowdown in the decay of western North Pacific tropical cyclones making landfall on the Asian continent. *Front. Earth Sci.* **9**, 749287 (2021).
9. Chen, J. et al. Changing impacts of tropical cyclones on East and Southeast Asian inland regions in the past and a globally warmed future climate. *Front. Earth Sci.* **9**, 769005 (2021).
10. Zhu, Y.-J. & Collins, J. M. Recent rebounding of the post-landfall hurricane wind decay period over the continental United States. *Geophys. Res. Lett.* **48**, e2020GL092072 (2021).
11. Wang, S. & Toumi, R. Recent migration of tropical cyclones toward coasts. *Science* **371**, 514–517 (2021).
12. Chan, K. T. F., Zhang, K., Wu, Y. & Chan, J. C. L. Landfalling hurricane track modes and decay. *Nature* **606**, E7–E11 (2022).
13. Li, L. & Chakraborty, P. Author Correction: Slower decay of landfalling hurricanes in a warming world. *Nature* **593**, E4–E11 (2021).
14. Li, L. & Chakraborty, P. Reply to: Landfalling hurricane track modes and decay. *Nature* **606**, E12–E15 (2022).
15. Phillipson, L. M. & Toumi, R. A physical interpretation of recent tropical cyclone post-landfall decay. *Geophys. Res. Lett.* **48**, e2021GL094105 (2021).
16. Schreck, C. J. III, Knapp, K. R. & Kossin, J. P. The impact of best track discrepancies on global tropical cyclone climatologies using IBTrACS. *Monthly Weather Rev.* **142**, 3881–3899 (2014).
17. Wu, L., Zhao, H., Wang, C., Cao, J. & Liang, J. Understanding of the effect of climate change on tropical cyclone intensity: a review. *Adv. Atmos. Sci.* **39**, 205–221 (2022).
18. Moon, I.-J., Kim, S.-H. & Chan, J. C. L. Climate change and tropical cyclone trend. *Nature* **570**, E3–E5 (2019).
19. Chan, K. T. F. Are global tropical cyclones moving slower in a warming climate? *Environ. Res. Lett.* **14**, 104015 (2019).
20. Zhou, T. et al. Why the western Pacific subtropical high has extended westward since the late 1970s. *J. Clim.* **22**, 2199–2215 (2009).
21. Landsea, C. W. & Franklin, J. L. Atlantic hurricane database uncertainty and presentation of a new database format. *Monthly Weather Rev.* **141**, 3576–3592 (2013).
22. Knapp, K. R., Kruk, M. C., Levinson, D. H., Diamond, H. J. & Neumann, C. J. The international best track archive for climate stewardship (IBTrACS). *Bull. Am. Meteorological Soc.* **91**, 363–376 (2010).
23. Hersbach, H. et al. The ERA5 global reanalysis. *Q. J. R. Meteorological Soc.* **146**, 1999–2049 (2020).
24. Kaplan, J. & DeMaria, M. A simple empirical model for predicting the decay of tropical cyclone winds after landfall. *J. Appl. Meteorol. Climatol.* **34**, 2499–2512 (1995).

## ACKNOWLEDGEMENTS

This study was supported by the National Key R&D Program of China (2019YFC1510400), the National Natural Science Foundation of China (41975052), the Innovation Group Project of the Southern Marine Science and Engineering Guangdong Laboratory (Zhuhai) (311021001), and the Guangdong Province Key Laboratory for Climate Change and Natural Disaster Studies (2020B1212060025).

## AUTHOR CONTRIBUTIONS

K.T.F.C. conceived the idea, performed the analysis, and wrote the manuscript. K.T.F.C. and J.C.L.C. contributed to the discussion and editing of the manuscript. K.Z. and Y.W. did data processing.

## COMPETING INTERESTS

The authors declare no competing interests.

## ADDITIONAL INFORMATION

**Supplementary information** The online version contains supplementary material available at <https://doi.org/10.1038/s41612-022-00320-z>.

**Correspondence** and requests for materials should be addressed to Kelvin T. F. Chan.

**Reprints and permission information** is available at <http://www.nature.com/reprints>

**Publisher's note** Springer Nature remains neutral with regard to jurisdictional claims in published maps and institutional affiliations.



**Open Access** This article is licensed under a Creative Commons Attribution 4.0 International License, which permits use, sharing, adaptation, distribution and reproduction in any medium or format, as long as you give appropriate credit to the original author(s) and the source, provide a link to the Creative Commons license, and indicate if changes were made. The images or other third party material in this article are included in the article's Creative Commons license, unless indicated otherwise in a credit line to the material. If material is not included in the article's Creative Commons license and your intended use is not permitted by statutory regulation or exceeds the permitted use, you will need to obtain permission directly from the copyright holder. To view a copy of this license, visit <http://creativecommons.org/licenses/by/4.0/>.

© The Author(s) 2022